PHYSICAL REVIEW E **91**, 010101(R) (2015)

Morphological evolution of domains in spinodal decomposition

Charu Datt,[1] Sumesh P. Thampi,[2] and Rama Govindarajan[1]
[1]*Centre for Interdisciplinary Sciences, Tata Institute of Fundamental Research, 21 Brundavan Colony, Narsingi, Hyderabad 500075, India*
[2]*Rudolf Peierls Centre for Theoretical Physics, 1 Keble Road, Oxford OX1 3NP, United Kingdom*
(Received 24 July 2014; revised manuscript received 18 December 2014; published 5 January 2015)

Domain growth in spinodal decomposition is usually described by a single time-evolving length scale. We show that the evolution of morphology of domains is nonmonotonic. The domains elongate rapidly at first and then, with the help of hydrodynamics, return to a more circular shape. The initial elongation phase does not alter with hydrodynamics. A small deviation from critical composition changes the morphology dramatically.

DOI: 10.1103/PhysRevE.91.010101 PACS number(s): 64.60.−i, 82.70.−y

Spinodal decomposition is observed in a binary fluid system when a homogeneous mixture of two fluids is quenched below the critical temperature so that it spontaneously demixes into regions containing each of its constituents [1]. This process occurs through the formation and growth of domains of the two phases. The long entwining structures in a 50:50 (also known as critical or symmetric) mixture and the dispersed droplets in an off-critical mixture (where one component dominates) are familiar images [2–8]. Following the dynamical scaling hypothesis, this structure has hitherto been characterized by a time-dependent length scale $L(t) \sim t^{\alpha}$, where α is the growth exponent [9]. With few exceptions [10–12], far less attention has been paid to the question of how the morphology of the domains evolves during spinodal decomposition and to the effect of hydrodynamics on this evolution and we address these questions in this paper.

Spinodal decomposition is now studied in a variety of systems such as in polymers [13], polymer colloid mixtures [14], gelation of protein solutions [15], crystallization facilitated by heterogeneous nucleation in interfaces [16], systems interfering with glass transitions [17], and active systems [18]. Novel structures can form in phase-separating mixtures, such as bicontinuous gels formed by the introduction of colloids into the mixture [19]. Nanoporous network formation during dealloying [20] and properties of alloys characterized using microstructure [21] are also based on spinodal decomposition effects. Surface-directed decompositions [22] and driven systems, e.g., by shear [23], are also active areas of research. A common theme among many of these studies is the evolution of the microstructure, which affects the macroscopic behavior and/or the physical properties. Our demonstration here that the anisotropy of the morphology evolves in time can prove to be important in this context.

Domain morphology has attracted attention in some previous studies [3–5,10–12]. Reference [3] highlights the differences arising due to change in the initial concentration of the components, while [4] describes the coalescence-induced growth of clusters. In [5] the authors describe variations in morphology of emerging domains with viscosity and diffusivity of the fluids and state that the dominant growth mechanism may be different at different length and time scales. Extensive analysis on morphology in terms of Euler characteristics, surface area, and distribution of curvatures is done in both two and three dimensions [10,11]. Robust scaling laws for these measures were also calculated, but the effects of hydrodynamics were not taken into account. Here we propose isoperimetric ratio as a measure of morphology and show how it nonmonotonically varies during the growth. Different measures such as interface length and connectivity (known as Minkowski functionals) were introduced in [12] that show nonmonotonic behavior with time. Percolating morphology is reported to enhance the separation process [24]. However, all these studies concentrated on the relation between morphology and the scale-invariance principle. In contrast, we characterize the morphology, quantify how it varies with time, and ask the question of how hydrodynamics affects its evolution.

In addition, our study may have implications in observations of the breakdown of scale invariance in spinodal decomposition. Such instances have been reported earlier; see, e.g., [4,8]. Simulations of [5] show such a breakdown, due to competition between various growth mechanisms and additional physics. Thus one may wonder about the validity of the assumption of a single length scale to characterize the system. Our simulations show that anisotropic morphology is prominent at very early times. This evolution of anisotropic morphology may also interfere with characteristic time-dependent length scales.

In this paper we offer the isoperimetric ratio as a good measure to characterize the morphology of domains. We show, surprisingly, that the morphology evolves nonmonotonically. On a short diffusive time scale, structures take on extremely elongated shapes, even in an off-critical mixture. On a longer time scale, dictated by capillary effects, isotropy is partially or completely regained. Our simulations show that the return to isotropy is very slow without hydrodynamics. The behavior is a strong function of mixture composition, especially near criticality.

To study the binary fluid system, we define an order parameter ψ, which describes the local concentration. The Cahn-Hilliard equation (CHE)

$$\partial_t \psi + \nabla \cdot (\mathbf{u}\psi) = \nabla \cdot (M \nabla \mu) \tag{1}$$

describes the evolution of this order parameter. The Navier-Stokes equation (NSE) describes the conservation of momentum

$$\rho(\partial_t \mathbf{u} + \mathbf{u} \cdot \nabla \mathbf{u}) = -\nabla \mathbf{p} + \eta \nabla^2 \mathbf{u} + \psi \nabla \mu \tag{2}$$

along with equation of continuity $\nabla \cdot \mathbf{u} = 0$. The additional stress term arising from the gradients in the order parameter represents the Laplace and Marangoni stresses acting on interfaces. In the above, p stands for the isotropic contribution of the pressure, η is the viscosity, and M is the mobility relating

the thermodynamic flux of ψ to the gradient of chemical potential $\nabla\mu$. [7,25].

If one may ascribe a single length scale to the dynamics, the following scaling applies. In the diffusive regime, i.e., at early times [9,26], fluid velocities are small enough to neglect the advective term in Eq. (1), reducing the equation to $\partial_t\psi \sim M\nabla^2\mu$. With the chemical potential as $\mu \sim \gamma/L$, where γ is the surface tension, we have $L(t) \sim (M\gamma)^{1/3}t^{1/3}$, a growth driven by mobility and surface tension. At intermediate times, i.e., during the viscous regime, hydrodynamics becomes important such that the viscous term in Eq. (2) dominates the inertial term. Neglecting contributions from other terms, the shear stress term balances the force due to the gradient in the chemical potential $\eta\nabla^2\mathbf{u} \sim \psi\nabla\mu$ so that $L(t) \sim \gamma t/\eta$, which is the linear growth law as predicted by Siggia [27]. This stage is followed by the inertial regime, when fluid inertia becomes more important than viscous stresses. Here Eq. (2) reduces to $\rho\partial_t\mathbf{u} \sim \psi\nabla\mu$. This gives $L(t) \sim (\gamma/\rho)^{1/3}t^{2/3}$, as predicted by Furukawa [28]. These scalings have been observed in various studies [2,29]. Mechanisms such as cluster diffusion and reaction affect the growth process [30]. Similarly, droplet interactions can be important as predicted by [31] and confirmed via extensive molecular dynamics simulations [32]. When inertial forces are large, questions about the role of turbulence in limiting the coarsening process are addressed with large-scale simulations [33].

Immediately after the quench, where hydrodynamics is not developed and nonlinearities can be neglected, Eq. (1) is linearly unstable to fluctuations, indicating phase separation. Beyond this initial phase, numerical solutions are often required due to the complexity of the governing equations (1) and (2). We use a hybrid lattice-Boltzmann (LB) algorithm to solve this system of coupled partial differential equations [34].

For critical quenches we set $\langle\psi\rangle = 0$. For off-critical quenches $\langle\psi\rangle = \psi_0$, where ψ_0 varies according to the required relative concentration of the two fluids. Simulations are performed on a two-dimensional domain of size 1024×1024 with periodic boundary conditions. All results that we report have been averaged over three runs. All quantities are expressed in LB units in this work. The following values of the parameters are fixed in all our runs: $A = -B = -0.0108$, $K = 0.0216$, and $M = 10$. We use $\eta = 3.34$ and $\eta = 0.17$ to simulate high- and low-viscosity fluids.

Simulations are performed for fluid mixtures of different properties and compositions. The growth rate observed in various cases is illustrated in Fig. 1. Here the domains are characterized by a length scale $L(t) = 2\pi\int S(k,t)dk/\int kS(k,t)dk$ defined as the inverse of the first moment of the circularly averaged structure factor $S(k,t) \equiv \langle\psi(\mathbf{k},t)\psi(-\mathbf{k},t)\rangle$, where $k = |\mathbf{k}|$ is the modulus of the wave vector in Fourier space and $\psi(\mathbf{k},t)$ represents the spatial Fourier transform of the order parameter [7]. The angular brackets denote an average over a shell in $\mathbf{k}$ space at fixed k. Various regimes of growth observed for a symmetric mixture are shown in Fig. 1(a). Solving the system with no flow for a symmetric mixture gives the exponent $\alpha = 1/3$ as expected and will be referred to as diffusive hereafter. When the NSE and CHE are coupled together we use $\eta = 3.34$ and $\eta = 0.17$ to simulate high- and low-viscosity fluids. These exhibit $\alpha \approx 1/2$ and $\alpha = 2/3$ growths and will be referred to as the intermediate and inertial cases, respectively. In asymmetric mixtures, additional growth mechanisms may be present, changing the growth exponents. This change is evident in Fig. 1(b), with deviation from the $2/3$ slope occurring earlier as the composition becomes more asymmetric. It is not possible to extract any clear exponent from these simulations to attribute the growth to any particular mechanism. However, we retain the nomenclature (diffusive vs inertial regimes) described in symmetric mixtures in asymmetric mixtures as well for the convenience of discussion in the following sections.

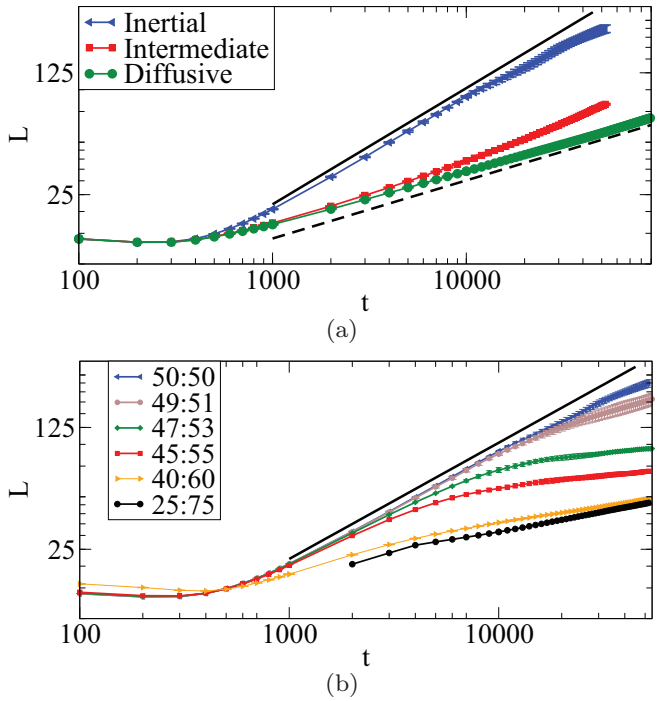

FIG. 1. (Color online) Domain growth characterized by a length scale $L(t)$ shown for (a) a symmetric mixture in the case of diffusive (no hydrodynamics), viscous (high viscosity $\eta = 3.34$), and inertial (small viscosity $\eta = 0.17$) regimes and (b) an asymmetric mixture with low viscosity. The solid black lines represent $t^{2/3}$ growth and the dashed line represents $t^{1/3}$ growth. Asymmetric mixtures grow significantly differently from this $2/3$ growth of symmetric mixtures in the inertial regime.

The effect of initial composition on the geometrical features of the separated phases during a spinodal decomposition process is illustrated in Fig. 2. Even a small difference from the 50:50 composition has a pronounced effect on the morphology of evolving domains. Snapshots from the simulations of a symmetric (50:50, $\psi_0 = 0$) and an off-symmetric (45:55, $\psi_0 = 0.1$) mixture are shown in Fig. 2 to make this evident. The initial growth in both the mixtures is via a diffusion process. This generates long and intertwined structures of phases as illustrated in the leftmost panels of Figs. 2(a) and 2(b). The characteristic width is much smaller than the characteristic length. In the off-critical mixture this anisotropy is lower. As time evolves, the domains grow. As has been observed in [4], the isolated droplets of the minority phase in the off-symmetric mixture grow via droplet coalescence also. In both cases, it is seen unambiguously that the anisotropy of the structures

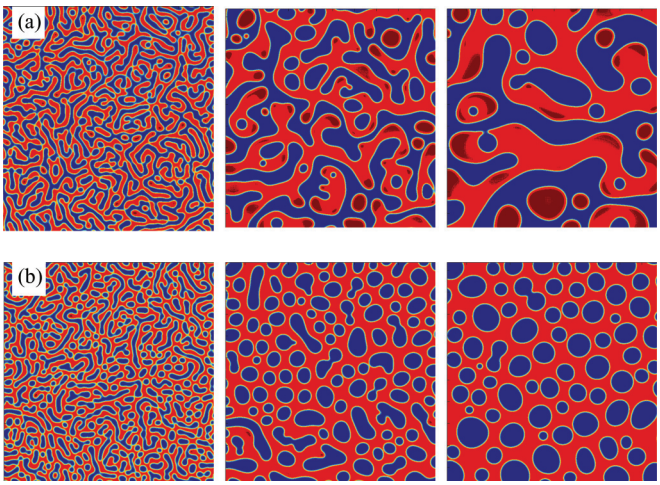

FIG. 2. (Color online) Spinodal decomposition in (a) a 50:50 and (b) a 45:55 binary mixture with time is illustrated. Evidently, the domains are highly anisotropic at early times. This anisotropy is carried forward in time in the 50:50 mixture, whereas a circular shape of the minority phase is restored at later times in the 45:55 mixture. The indicated length is in simulation units.

(observe the width-to-length ratio) evolves with time, but in different ways.

To quantify the morphology, we first identify and label the clusters [3,4] of one of the component fluids using a Hoshen-Kopelman algorithm [35], here, on a grid made up of cells across the computational domain, where each cell is either occupied or unoccupied. Using the algorithm we separate clusters of the two fluids and calculate associated geometrical quantities. To measure the anisotropy, we define the isoperimetric ratio [36] of each domain

$$Q \equiv \frac{P^2}{4\pi A},$$

where A is its area and P its perimeter. For a circular lobe $Q = 1$, whereas $Q > 1$ for any other shape. The greater the deviation from a circle, the higher the value of Q. For very elongated and branched domains, this ratio gives a measure of the length of the interface per unit area of the separated phase. The average isoperimetric ratio $\langle Q \rangle$ is obtained by averaging Q over space and over different realisations.

In Fig. 3(a) we plot the average isoperimetric ratio with time for different compositions, i.e., different ψ_0. The anisotropy in morphology, as measured by $\langle Q \rangle$, for all quenches except the most asymmetric (25:75 mixture), first increases and then decreases until it equilibrates to a value far lower than the maximum. This value is close to 1 for off-symmetric quenches, whereas for symmetric quenches at long times $\langle Q \rangle \sim 2$. The initial phase of increasing elongation of structures is also the phase of rapid growth of the clusters. Beyond this point, the number of clusters does not change much. Initially, the growth of the structures occurs preferentially at the ends rather than on the long sides. The elongated structures seen at the end of this growth phase then evolve towards a more circular geometry, thus giving a nonmonotonic variation of the isoperimetric ratio. We note that though $\langle Q \rangle$ grows only for a short time, this growth is decisive in determining the morphology of domains at later times.

Remarkably, even for as little a composition variation as to 49:51 ($\psi_0 = 0.05$) from a 50:50 ($\psi_0 = 0$) mixture, there is a substantial difference in the isoperimetric ratio. In other words, even a small asymmetry in composition results in domain shapes that are far less anisotropic. The peak value of $\langle Q \rangle$ decreases with the decrease in the amount of the minority phase. The 25:75 mixture evolves very slowly at early times. Once formed, domains of the minority phase remain close to a circular shape throughout their evolution.

To understand the anisotropic growth consider a domain in the shape of a stadium of width w as shown in Fig. 4. At early times, diffusive mechanisms dominate and the driving term in Eq. (1) may be estimated as $\sim M\mu/l^2$ in the flat portions of the domain, where l is the interfacial thickness. However, over a region of size $O(w)$ containing the semicircular caps at both ends, this term scales as $M\mu(1/l^2 + 2/lw)$ because $\nabla^2 \equiv \frac{d^2}{dr^2} + \frac{1}{r}\frac{d}{dr}$ in polar coordinates. Thus the ends grow faster than the flat portion. Once the width w becomes very large compared to the interfacial thickness, the difference becomes negligible and a return to isotropy is attempted. Thus a nonmonotonic shape factor accrues.

In the diffusive regime, $w \sim (M\gamma)^{1/3}t^{1/3}$ [9,26]. So when M, γ, and l are kept fixed, the time at which the maximum

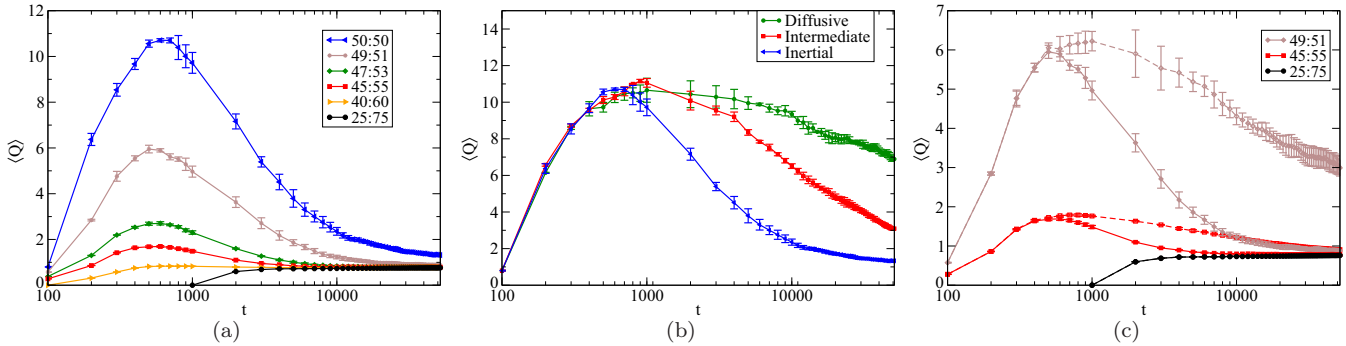

FIG. 3. (Color online) Variation of $\langle Q \rangle$ with time during spinodal decomposition shown for (a) various relative compositions of the two fluids in the inertial regime and (b) inertial, intermediate, and diffusive regimes of a symmetric quench. (c) Comparison between diffusive (dashed lines) and inertial (solid lines) cases for three different compositions. Hydrodynamics always helps in imparting a compact structure, but becomes less important for mixtures farther from criticality.

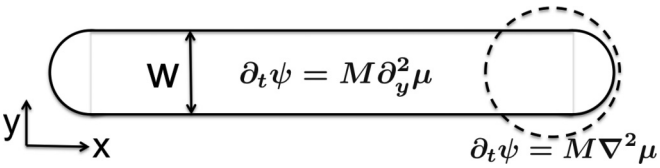

FIG. 4. Diffusion in a region of $O(w)$ is much stronger than elsewhere in a stadium-shaped domain as long as the relevant length scale for diffusion is comparable to the domain size w.

in $\langle Q\rangle$ occurs must be independent of the composition. This may be verified in Fig. 3, where these parameters are fixed. When these parameters are varied (not shown), we find that the maximum is shifted accordingly. It is of interest to note that the anisotropic growth of clusters, especially at early times, reveals the differently evolving length scales and can affect the measured exponent α.

The effect of hydrodynamics on the morphology evolution is examined in Fig. 3(b) for symmetric quenches. In the diffusion-controlled initial regime, hydrodynamics does not affect spinodal dynamics and structures are allowed to reach their maximal elongation. Without hydrodynamics, emerging domains remain very elongated even after long times. However, the return to isotropy is dramatically accelerated by hydrodynamics. In the inertial regime when capillary flows are large, i.e., viscosity is small, isotropy is regained. A similar behavior is displayed by asymmetric quenches of moderate composition, as can be seen in Fig. 3(c). However, quenches far from critical seem to be affected little by the hydrodynamics.

We now show that shape is important in determining the rate of growth. If there are $n(t)$ clusters of a given phase, we may define the average area and average perimeter of a cluster respectively by

$$\tilde{A} = \frac{A_{\rm tot}}{n(t)}, \quad \tilde{P} = \frac{P_{\rm tot}}{n(t)}, \tag{3}$$

where $A_{\rm tot}$ and $P_{\rm tot}$ are the total area and perimeter of all clusters of a given phase, respectively. In asymmetric quenches, we evaluate these for the minor phase. Mass conservation ensures that $A_{\rm tot}$ is a constant, so $\tilde{A}$ is inversely proportional to $n(t)$. We may calculate $r = (1/\tilde{P})(d\tilde{A}/dt)$ as a measure of the growth rate of a cluster. This is plotted vs $\langle Q\rangle$ in Fig. 5. Here time increases in the downward direction on a given curve. The growth rate is seen to be a monotonically decreasing function of time, with the fastest growth rates at initial times. By the time the maximum in isoperimetric ratio is attained, growth rates have dropped by about an order of magnitude. After this, structures do not grow much in size. Consistent with this, the change in the number of structures slows down as well. The large difference between isoperimetric ratios of the cases with and without hydrodynamics in each case at a given growth rate shows that the hydrodynamics does not affect the number or size of structures as much as it affects the shape. If scaled by the maximum in $\langle Q\rangle$, all the curves overlap each other (not shown), establishing the connection between shape and growth rate. However, this dependence of growth rate on morphology is a nontrivial effect and isolating it from other mechanisms warrants further study.

A clarification of the growth rate in Fig. 5 is in order here. In this figure, the same $\langle Q\rangle$ does not mean the same

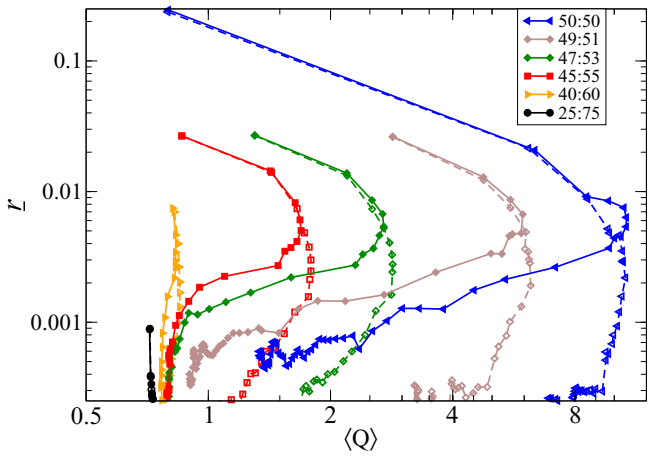

FIG. 5. (Color online) Cluster growth rate as a function of isoperimetric ratio during spinodal decomposition of various compositions for the inertial (solid line) and diffusive (dashed line) cases. Time runs from top to bottom, indicating fastest cluster growth at early times, until $\langle Q\rangle$ reaches its maximum in each case. The same $\langle Q\rangle$ does not mean the same stage of evolution across various cases.

stage of evolution for different compositions. The highest growth rate is exhibited by the symmetric mixture only. Comparison of growth rates across different compositions, if required, should be done in conjunction with Fig. 3(a). It should also be noted that, for asymmetric mixtures discussed here, growth may not be decisively controlled by diffusion or inertial hydrodynamics, but mechanisms such as droplet collisions (see, e.g., [32]) can be important. The comparisons between diffusive and inertial cases in Figs. 3(c) and 5 are really to highlight the role of hydrodynamics in morphological evolution than to characterize underlying mechanisms of growth. The morphology in turn can affect the growth though. As mentioned earlier, further attention is needed to separate out the effects of morphology alone.

To summarize, we have carried out extensive lattice-Boltzmann simulations to simulate spinodal decomposition. We show, surprisingly, that morphology evolves nonmonotonically for a range of compositions. An initial phase of rapid elongation of structures is followed by a phase where hydrodynamics achieves a return to isotropy. A physical argument for this nonmonotonicity is proposed. The actual elongation achieved strongly depends on composition, especially close to the critical composition. The rate of return to isotropy is much faster at low viscosity. If we describe structures in terms of the evolution of a single length scale, our results are consistent with behavior observed before, but our main point is that a single length is insufficient to describe spinodal decomposition. If characterized by a single length scale, one would only find this increasing with time, whereas along the elongated direction we actually find a reduction at later times. There are several situations, including those with industrial relevance, where we believe this anisotropic morphology will be seen, e.g., (i) spinodal dewetting where the presence of the solid substrate will dampen the momentum quickly and hence impede the return to isotropy and (ii) spinodal decomposition of polymers and alloys where high viscosity should prevent the return to isotropy. Where physical properties are crucially

related to the microstructure of the material, the evolution of this anisotropy will affect the answer. An extension to three-dimensional systems may be interesting and is set aside for the future.

The authors gratefully acknowledge discussions with Ronojoy Adhikari for the development of LB code and thank Jawaharlal Nehru Centre for Advanced Scientific Research, Bangalore where this work began.

[1] J. W. Cahn, J. Chem. Phys. **42**, 93 (1965).
[2] M. San Miguel, M. Grant, and J. D. Gunton, Phys. Rev. A **31**, 1001 (1985); H. Furukawa, Physica A **204**, 237 (1994).
[3] J. E. Farrell and O. T. Valls, Phys. Rev. B **43**, 630 (1991).
[4] G. Leptoukh, B. Strickland, and C. Roland, Phys. Rev. Lett. **74**, 3636 (1995).
[5] A. J. Wagner and J. M. Yeomans, Phys. Rev. Lett. **80**, 1429 (1998).
[6] H. Furukawa, Phys. Rev. E **61**, 1423 (2000).
[7] V. M. Kendon, M. E. Cates, I. Pagonabarraga, J.-C. Desplat, and P. Bladon, J. Fluid Mech. **440**, 147 (2001).
[8] J. Chin and P. V. Coveney, Phys. Rev. E **66**, 016303 (2002).
[9] A. Bray, Adv. Phys. **43**, 357 (1994); Philos. Trans. R. Soc. London, Ser. A **361**, 781 (2003).
[10] M. Fiałkowski, A. Aksimentiev, and R. Hołyst, Phys. Rev. Lett. **86**, 240 (2001).
[11] M. Fiałkowski and R. Hołyst, Phys. Rev. E **66**, 046121 (2002).
[12] K. R. Mecke and V. Sofonea, Phys. Rev. E **56**, R3761 (1997).
[13] P. G. de Gennes, J. Chem. Phys. **72**, 4756 (1980); K. Asadi, H. J. Wondergem, R. S. Moghaddam, C. R. McNeill, N. Stingelin, B. Noheda, P. W. M. Blom, and D. M. de Leeuw, Adv. Funct. Mater. **21**, 1887 (2011).
[14] E. A. G. Jamie, R. P. A. Dullens, and D. G. A. L. Aarts, J. Chem. Phys. **137**, 204902 (2012); A. Winkler, P. Virnau, K. Binder, R. G. Winkler, and G. Gompper, *ibid.* **138**, 054901 (2013).
[15] T. Gibaud and P. Schurtenberger, J. Phys.: Condens. Matter **21**, 322201 (2009).
[16] M. K. Mitra and M. Muthukumar, J. Chem. Phys. **132**, 184908 (2010).
[17] V. Testard, L. Berthier, and W. Kob, Phys. Rev. Lett. **106**, 125702 (2011).
[18] R. Wittkowski, A. Tiribocchi, J. Stenhammar, R. J. Allen, D. Marenduzzo, and M. E. Cates, Nat. Commun. **5**, 4351 (2014).
[19] K. Stratford, R. Adhikari, I. Pagonabarraga, J.-C. Desplat, and M. E. Cates, Science **309**, 2198 (2005).
[20] J. Erlebacher, M. J. Aziz, A. Karma, N. Dimitrov, and K. Sieradzki, Nature (London) **410**, 450 (2001).
[21] O. Soriano-Vargas, E. O. Avila-Davila, V. M. Lopez-Hirata, N. Cayetano-Castro, and J. L. Gonzalez-Velazquez, Mater. Sci. Eng. A **527**, 2910 (2010); S. Sheibani, S. Heshmati-Manesh, A. Ataie, A. Caballero, and J. Criado, J. Alloys Compd. **587**, 670 (2014).
[22] U. Thiele, M. G. Velarde, and K. Neuffer, Phys. Rev. Lett. **87**, 016104 (2001); P. K. Jaiswal, S. Puri, and S. K. Das, Europhys. Lett. **97**, 16005 (2012); A. M. Higgins and R. A. Jones, Nature (London) **404**, 476 (2000).
[23] A. J. Wagner and J. M. Yeomans, Phys. Rev. E **59**, 4366 (1999); J. Liu, L. Dedè, J. A. Evans, M. J. Borden, and T. J. Hughes, J. Comput. Phys. **242**, 321 (2013).
[24] S. Roy and S. K. Das, J. Chem. Phys. **139**, 044911 (2013)
[25] P. M. Chaikin and T. C. Lubensky, *Principles of Condensed Matter Physics* (Cambridge University Press, Cambridge, 2000); J. J. S. Rowlinson and B. Widom, *Molecular Theory of Capillarity* (Dover, Mineola, 2002).
[26] T. Lookman, Y. Wu, F. J. Alexander, and S. Chen, Phys. Rev. E **53**, 5513 (1996).
[27] E. D. Siggia, Phys. Rev. A **20**, 595 (1979).
[28] H. Furukawa, Phys. Rev. A **31**, 1103 (1985).
[29] P. V. Coveney and K. E. Novik, Phys. Rev. E **54**, 5134 (1996); E. Velasco and S. Toxvaerd, Phys. Rev. Lett. **71**, 388 (1993); W. R. Osborn, E. Orlandini, M. R. Swift, J. M. Yeomans, and J. R. Banavar, *ibid.* **75**, 4031 (1995); R. B. Rybka, M. Cieplak, and D. Salin, Physica A **222**, 105 (1995).
[30] K. Binder and D. Stauffer, Phys. Rev. Lett. **33**, 1006 (1974); K. Binder, Phys. Rev. B **15**, 4425 (1977).
[31] H. Tanaka, J. Chem. Phys. **103**, 2361 (1995); **105**, 10099 (1996); **107**, 3734 (1997).
[32] S. Roy and S. K. Das, Phys. Rev. E **85**, 050602 (2012); Soft Matter **9**, 4178 (2013).
[33] P. Perlekar, R. Benzi, H. J. H. Clercx, D. R. Nelson, and F. Toschi, Phys. Rev. Lett. **112**, 014502 (2014).
[34] O. Henrich, D. Marenduzzo, K. Stratford, and M. E. Cates, Phys. Rev. E **81**, 031706 (2010); S. P. Thampi, I. Pagonabarraga, and R. Adhikari, *ibid.* **84**, 046709 (2011).
[35] J. Hoshen and R. Kopelman, Phys. Rev. B **14**, 3438 (1976).
[36] S. P. Thampi, R. Adhikari, and R. Govindarajan, Langmuir **29**, 3339 (2013).